Conformational Determinants of Agonist versus Antagonist Properties of [D-Pen^2,D-Pen^5]Enkephalin (DPDPE) Analogs at Opioid Receptors. Comparison of X-ray Crystallographic Structure, Solution ^{1}H NMR Data, and Molecular Dynamic Simulations of [L-Ala^3]DPDPE and [D-Ala^3]DPDPE

Nathan Collins,[†,§] Judith L. Flippen-Anderson,[‡] Ronald C. Haaseth,[†,∥] Jeffery R. Deschamps,[‡] Clifford George,[‡] Katalin Kövér,[†,⊥] and Victor J. Hruby*[,†]

Contribution from the Department of Chemistry, University of Arizona, Tucson, Arizona 85712, and Laboratory for the Structure of Matter, Code 6030, Naval Research Laboratory, Washington, DC 20375

Received September 11, 1995[⊗]

Abstract: c-[D-Pen^2,D-Pen^5]enkephalin (DPDPE, **1**) is a cyclic, constrained, highly potent, δ opioid receptor selective peptide agonist. Substitution of Gly^3 with L-Ala in DPDPE to give [L-Ala^3]DPDPE (**2**) has been shown to produce a peptide with much greater δ receptor binding selectivity than DPDPE itself. However [L-Ala^3]DPDPE is only a partial agonist in *in vivo* antinociception and actually was found to potently *antagonize* the antinociceptive effects of DPDPE at δ receptors in the brain. In comparison, [D-Ala^3]DPDPE (**3**) is a weak and poorly selective δ agonist. In an effort to correlate the biological profiles of these peptides with secondary structure, [L-Ala^3]DPDPE and [D-Ala^3]-DPDPE were studied by X-ray crystallography and ^{1}H and ^{13}C NMR in DMSO solution. Crystals of both peptides were obtained using vapor diffusion techniques. [L-Ala^3]DPDPE crystallizes in the monoclinic space group *C*2 with cell dimensions $a = 36.35(1)$ Å, $b = 19.737(4)$ Å, $c = 28.16(1)$ Å, $\beta = 129.07(2)°$, and $V = 15688(9)$ Å^3. The asymmetric unit contains four peptide molecules and approximately 20 water molecules, giving a calculated density of 1.274 g cm^{-3}. The conformation of all four independent [L-Ala^3]DPDPE molecules is essentially the same. [D-Ala^3]-DPDPE crystallizes in the monoclinic space group $P2_1$ with cell dimensions $a = 12.271(2)$ Å, $b = 9.600$(a) Å, $c = 18.750(4)$ Å, $\beta = 103.56(2)°$, and $V = 2147.2(7)$ Å^3. The asymmetric unit contains one peptide molecule and 10 molecules of water, giving a calculated density of 1.298 g cm^{-3}. Comparison of these X-ray structures with the crystal structure previously reported for DPDPE indicates that there are differences in the disulfide bond region for all three peptides. ROEs determined about the disulfide regions of **1**−**3** in solution are indicative of a high degree of conformational interconversion, while heteronuclear coupling constants between the D-Pen^{2,5} Hα and Cγ,γ' carbons indicate a strong preference for a gauche (+) χ^1 angle in **2**. The backbone conformations of DPDPE and [D-Ala^3]-DPDPE in the X-ray structures are virtually identical, while in [L-Ala^3]DPDPE, there is a rotation of approximately 160° about both ψ^2 and φ^3 compared to DPDPE which has the effect of rotating this amide group approximately 180° relative to DPDPE. The solution NMR data for the peptide backbone conformations of **2** and **3** are mainly consistent with their X-ray structures. However, MD simulation of all three compounds, starting with the geometries of their X-ray structures, indicates that by comparison of observed and predicted ROE intensities an equilibrium between these conformations is likely in solution. The "DPDPE-like" conformation for [L-Ala^3]DPDPE is however significantly higher in energy than the X-ray structure reported here and, thus, is predicted to be less populated in solution and in receptor binding. It is concluded that the X-ray structure of DPDPE represents an agonist conformation for this peptide at the δ opioid receptor and that the corresponding X-ray structure of [L-Ala^3]DPDPE represents an antagonist conformation due to the differences in conformation between positions 2 and 3. Considerations on the structural implications of this conformational difference on receptor binding are discussed.

Introduction

The search for the bioactive conformations of the opioid peptides at specific opioid receptors has continued for the last 20 years and is still a matter of intensive study in many groups. The difficulties in the pursuit of this goal are 2-fold. The highly flexible nature of the linear natural peptides such as leucine and methionine enkephalin make them virtually structureless in solution, and several different conformations (extended, single bend, double bend) have been observed in X-ray crystallography studies.[1,2] In turn, the flexibility of these peptides renders them relatively nonselective in binding to the commonly accepted μ, δ, and κ opioid receptors.[3−6] This problem recently has been

* To whom correspondence should be addressed.
† University of Arizona.
‡ Naval Research Laboratory.
§ Current address: Arris Pharmaceutical Corp., 385 Oyster Point Blvd, Suite 3 South, San Francisco, CA 94080.
∥ Current address: Protein Structure Facility, 2560 MSRB-2, Box 0674, University of Michigan, 1150 W. Medical Center Drive, Ann Arbor, MI 48109.
⊥ Current address: Department of Organic Chemistry, L. Kossuth University, Debrecen, P.O. Box 20, Hungary H-4010.
⊗ Abstract published in *Advance ACS Abstracts,* February 1, 1996.

(1) Karle, I. L.; Karle, J.; Mastaropollo, D.; Camerman, A.; Camerman, H. *Acta Crystallogr*. **1983**, *B39*, 623−637.
(2) (a) Griffin, J. F.; Langs, D. A.; Smith, G. D.; Blundell, T. L.; Tickle, I. J.; Bederkar, S. *Proc. Natl. Acad. Sci. U.S.A.* **1986**, *83*, 3272−3275. (b) Aubry, A.; Birlirakis, N.; Sakarellos-Daitsiotis, M.; Sakarellos, C.; Marraud, M. *Biopolymers* **1989**, *28*, 27−40.

0002-7863/96/1518-2143$12.00/0

complicated by the discovery of subtypes of these receptors with presumably subtle differences in binding requirements.[7−13] A central theme in many modern structure function studies is thus the incorporation of conformational and topographical constraints into such linear peptides in order to force the structure into the binding conformation of one particular receptor, thus making it highly selective for that receptor.[14−17] The success of such an approach is heightened by the fact that the constrained conformation of the resulting ligand is often more readily deducible by spectroscopic analyses such as solution NMR and X-ray crystallography, which can facilitate the iterative synthesis of further peptide or peptidomimetic analogs targeted for improved binding and selectivity.

An early example of the success of this approach was the disulfide cyclized peptide analog of Leu^5 (or Met^5) enkephalin, [D-Pen^2,D-Pen^5]enkephalin (H-Tyr-D-Pen-Gly-Phe-D-Pen-OH (**1**), DPDPE, Figure 1; Pen = penicillamine).[18] This cyclic constrained ligand is a potent opioid agonist which is selective for the δ receptor. Recent studies have indicated that DPDPE is in fact selective for δ_1 subtype receptors, while the naturally occurring deltorphin peptides are δ_2 selective agonists.[7] With the conformational freedom of this peptide limited by the cyclization, several studies have attempted to determine the "bioactive" conformation of DPDPE. Studies using parameters from ^{1}H NMR in water[19−21] and DMSO[21] have indicated that despite the cyclic constraint in **1** there is still rapid interchange between an ensemble of local conformations in solution.

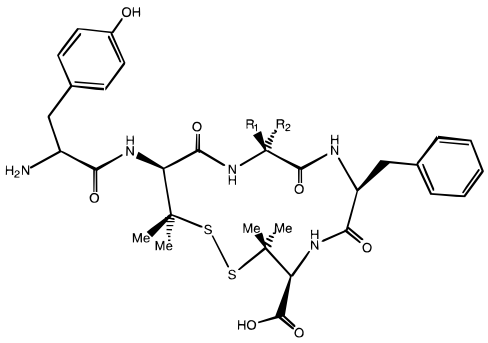

R_1,R_2 = H	H - Tyr - D-Pen - Gly - Phe - D-Pen - OH	DPDPE	**1**
R_1=Me,R_2=H	H - Tyr - D-Pen - L-Ala - Phe - D-Pen - OH	[L-Ala^3]DPDPE	**2**
R_1=H,R_2=Me	H - Tyr - D-Pen - D-Ala - Phe - D-Pen - OH	[D-Ala^3]DPDPE	**3**

Figure 1. Structures of [D-Pen^2,D-Pen^5]enkephalin (**1**), [D-Pen^2,L-Ala^3,D-Pen^5]enkephalin (**2**), and [D-Pen^2,D-Ala^3,D-Pen^5]enkephalin (**3**).

Several molecular mechanics[19,21−25] and dynamics[26,27] studies also have been reported which have reached various conclusions about the conformational preferences of DPDPE in solution and when bound to opioid receptors.[28] These investigations culminated in the recently reported X-ray structure of DPDPE.[29] The highly hydrated crystallized form of this peptide was found to share conformational features indicated from solution NMR studies and molecular mechanics studies which predicted its conformation when bound to the δ opioid receptor. Aspects of the X-ray structure of DPDPE were thus suggested to approximate the "bioactive" agonist conformation of DPDPE.[29]

In the light of these studies, the functional group and stereochemical requirements of position 3 replacements in DPDPE were reported recently.[30] Substitution of Gly^3 with L-Ala to give [L-Ala^3]DPDPE (**2**) produced a peptide with much greater selectivity in central (brain) receptor binding assays and peripheral bioassay than DPDPE itself (ratio of μ/δ binding for **1** was 620 versus 11 000 for **2**). However, [L-Ala^3]DPDPE proved to be only a partial agonist in *in vivo* antinociception and actually was found to potently *antagonize* the antinociceptive effects of DPDPE at δ receptors in the brain.[30] In comparison, [D-Ala^3]DPDPE (**3**) was a weak and poorly selective δ agonist at peripheral and brain receptors. These surprising results prompted us to determine the conformations of **2** and **3** by solution NMR and X-ray crystallography. Correlation of the data from these studies with the X-ray structure of DPDPE by molecular dynamic simulations not only gave direct information on the conformational ensemble in solution for these peptides but also produced highly specific conformational details on the importance of the backbone structure of DPDPE and its analogs for δ receptor agonist versus antagonist binding.

(3) Martin, W. R.; Easdes, C. G.; Thompson, J. A.; Hupper, R. E.; Hilbert, P. E. *J. Pharmacol. Exp. Ther.* **1976**, *197*, 517−524.
(4) Lord, J. A.; Waterfield, A. A.; Hughes, J.; Kosterlitz, H. W. *Nature* **1977**, *267*, 495−499.
(5) Wolozin, B. L.; Pasternak, G. W. *Proc. Acad. Sci. U.S.A.* **1981**, *78*, 6181−6185.
(6) Rapaka, R. S.; Barnett, G.; Hawks, R. L., Eds. *Opioid Peptides: Medicinal Chemistry*; NIDA Research Monograph 69; National Institute in Drug Abuse: Rockville, MD, 1986.
(7) Mattia, A.; Farmer, S. C.; Takemori, A. E.; Sultana, M.; Portoghese, P. S.; Mosberg, H. I.; Bowen, W. D.; Porreca, F. *J. Pharmacol. Exp. Ther.* **1992**, *260*, 518−525.
(8) Negri, L.; Potenza, R. L.; Corsi, R.; Melchiorri, P. *Eur. J. Pharmacol.* **1991**, *196*, 335−336.
(9) Xu, H.; Ni, Q.; Jacobson, A. E.; Rice, K. C.; Rothman, R. B. *Life Sci.* **1991**, *49*, PL-141−PL-146.
(10) Jiang, Q.; Takemori, A. E.; Sultana, M.; Portoghese, P. S.; Bowen, W. D.; Mosberg, H. I.; Porreca, F. *J. Pharmacol. Exp. Ther.* **1991**, *257*, 1069−1075.
(11) Mattia, A.; Vanderah, T.; Mosberg, H. I.; Porreca, F. *J. Pharmacol. Exp. Ther.* **1991**, *258*, 583−587.
(12) Sofouoglu, M.; Portoghese, P. S.; Takemori, A. E. *J. Pharmacol. Exp. Ther.* **1991**, *257*, 676−680.
(13) Horan, P. J.; Wild, K. D.; Misicka, A.; Lipowski, A. W.; Haaseth, R. C.; Hruby, V. J.; Weber, S. J.; Davis, T. P.; Yamamura, H. I.; Porreca, F. *J. Pharmacol. Exp. Ther.* **1993**, *265*, 896−902.
(14) Hruby, V. J. In *Perspectives in Peptide Chemistry*; Eberle, A., Guiger, R., Wieland, T., Eds.; S. Karger: Basel, Switzerland, 1981; pp 207−220.
(15) Marshall, G. R.; Cramer, D. D. *Trends Pharmacol. Sci.* **1988**, *9*, 285−288.
(16) Freidinger, R.; Veber, D. In *Conformationally Directed Drug Design, Peptides and Nucleic Acids on Templates of Targets*; Vida, J. A., Gordon, M., Eds.; ACS Symposium Series 251; American Chemical Society: Washington, DC, 1984; pp 169−187.
(17) Hruby, V. J. In *Conformationally Directed Drug Design Peptides and Nucleic Acids on Templates of Targets*; Vida, J. A., Gordon, M., Eds.; ACS Symposium Series 251; American Chemical Society: Washington, DC, 1984; pp 9−27.
(18) Mosberg, H. I.; Hurst, R.; Hruby, V. J.; Gee, K.; Yamamura, H. I.; Galligan, J. J.; Burks, T. F. *Proc. Natl. Acad. Sci. U.S.A.* **1983**, *80*, 5871−5874.
(19) Hruby, V. J.; Kao, L. F.; Pettit, B. M.; Karplus, M. *J. Am. Chem. Soc.* **1988**, *110*, 3351−3359.
(20) Mosberg, H. I.; Sobczyyk-Kojiro; Subramanian, P.; Crippen, G.; Ramalingam, M. K.; Woodward, R. W. *J. Am. Chem. Soc.* **1990**, *112*, 822−829.
(21) Nikiforovich, G.; Prakash, O.; Gehrig, C. A.; Hruby, V. J. *Int. J. Pept. Protein Res.* **1993**, *41*, 347−361.
(22) Chew, C.; Villar, H. O.; Loew, G. H. *Biopolymers* **1993**, *33*, 647−657.
(23) Froimowitz, M.; Hruby, V. J. *Int. J. Pept. Protein Res.* **1989**, *34*, 88−96.
(24) Froimowitz, M. *Biopolymers* **1990**, *30*, 1011.
(25) Wilkes, B. C.; Schiller, P. W. *J. Comput.-Aided Mol. Des.* **1991**, *5*, 293−302.
(26) Pettitt, B. M.; Matsunaga, T.; Al-Obeidi, F.; Gehrig, C.; Hruby, V. J.; Karplus, M. *Biophys. J.* **1991**, *60*, 1540−1544.
(27) Smith, P. E.; Pettitt, B. M. *Biopolymers* **1992**, *32*, 1623−1629.
(28) Nikiforovich, G.; Hruby, V. J.; Prakash, O.; Gehrig, C. A. *Biopolymers* **1991**, *31*, 941−955.
(29) Flippen-Anderson, J. L.; Hruby, V. J.; Collins, N.; George, C.; Cudney, B. *J. Am. Chem. Soc.* **1994**, *116*, 7523−7531.
(30) Haaseth, R. C.; Horan, P. J.; Bilsky, E. J.; Davis, P.; Zalewska, T.; Slaninova, J.; Yamamura, H. I.; Weber, S. J.; Davis, T. P.; Porreca, F.; Hruby, V. J. *J. Med. Chem.* **1994**, *37*, 1572−1577.

Table 1. Crystal Data and Structure Refinement Parameters for [L-Ala^3]- and [D-Ala^3]DPDPE

	[L-Ala]DPDPE	[D-Ala]DPDPE
	Crystal Data	
emp form	$4(C_{31}H_{41}N_5O_7S_2)\cdot 20.5H_2O$	$C_{31}H_{41}N_5O_7S_2\cdot 10H_2O$
crystal habit	clear colorless rods	clear colorless rods
crystal size (mm)	$0.04 \times 0.07 \times 0.66$	$0.08 \times 0.10 \times 0.45$
crystal system	monoclinic	monoclinic
space group	$C2$	$P2_1$
unit cell dimens	$a = 36.36(1)$ Å, $b = 19.737(4)$ Å, $c = 28.16(1)$ Å, $\alpha = 90°$, $\beta = 129.07(2)°$, $\gamma = 90°$	$a = 12.271(2)$ Å, $b = 9.600(2)$ Å, $c = 18.750(4)$ Å, $\alpha = 90°$, $\beta = 103.56(2)°$, $\gamma = 90°$
volume (Å^3)	15688(9)	2147.2(7)
Z	4	2
density (calcd) (g/cm^3)	1.274	1.298
form wt/F(000)	3008.5/6420	839.0/898
	Data Collection	
wavelength (Å)/temp (K)	1.54178/243(2)	1.54178/243(2)
scan type	$\theta/2\theta$	$\theta/2\theta$
scan speed	variable depending upon intensity	
index ranges	$-36 \le h \le 11$; $0 \le k \le 19$; $-21 \le l \le 27$	$0 \le h \le 13$; $0 \le k \le 10$; $-19 \le l \le 19$
no. of reflns colld	9382	3046
no. of ind reflns	8470 ($R_{int} = 0.0235$)	2828 ($R_{int} = 0.0387$)
no. of observed reflns	5770 ($I > 2\sigma I$)	2146 ($I > 2\sigma I$)
resolution	0.9	0.9
	Refinement	
method	full-matrix least-squares on F^2	
no. of data/restraints/params	8449/64/1789	2732/279/506
goodness-of-fit on F^2	1.058	1.035
final R indices [$I > 2\sigma(I)$]	$R1 = 0.0984$, w$R2 = 0.2317$	$R1 = 0.0900$, w$R2 = 0.1978$
R indices (all data)	$R1 = 0.1452$, w$R2 = 0.2867$	$R1 = 0.1241$, w$R2 = 0.2442$
R_{free} (85 data)		0.142
abs struct param	0.0(5)	0.0(7)
extinction coeff	0.0023(2)	
largest diff peak and hole (e Å^{-3})	0.566 and −0.448	0.508 and −0.379

Methods

Synthesis. [L-Ala^3]DPDPE and [D-Ala^3]DPDPE were synthesized by standard Merrifield solid phase peptide synthetic protocols and purified by preparative reverse phase (RP) HPLC (high-pressure liquid chromatography) as previously described.[30] Purity was assessed by analytical RP-HPLC and thin layer chromatography.

Crystallization. Stock solutions of [L-Ala^3]DPDPE and [D-Ala^3]-DPDPE (8.3 mg/mL in 16% acetic acid and 13 mg/mL in water, respectively) were filtered using a Millipore Ultrafree μC Durapore 0.22 μm filter and stored at room temperature. Crystals were grown by vapor diffusion techniques using sitting drops in wells of Linbro tissue culture plates. Diffraction quality crystals of [L-Ala^3]DPDPE were grown over a 4-week period from drops containing 10 μL of stock solution and 10 μL of reservoir solution over a 1000 μL reservoir containing 7% w/v PEG 8000. Diffraction quality crystals of [D-Ala^3]-DPDPE were grown by microseeding droplets containing 15 μL of stock solution and 15 μL of reservoir solution over 1000 μL reservoirs containing 25% w/v PEG 8000. The microseeds were introduced after the drops had been allowed to stand for 24 h. Crystals grew over a 7-day period. Both crystallizations occurred at a constant temperature of 22 °C in a Napco Model 2900 incubator.

Structure Solution and Refinement. Crystals were prepared for data collection by transferring them from their mother liquor into high-viscosity microscope oil (Type NVH, Cargille). They were then mounted on a glass rod while still in the oil and transferred immediately to the liquid nitrogen cold stream (−60 °C) on the diffractometer. X-ray diffraction data for both peptides were collected on an automated four-circle diffractometer (Siemens R3m/V) equipped with an incident beam graphite monochromator. Three reflections, used as standards, were monitored after every 97 new measurements and showed random fluctuations of ±2.5%. Data were corrected for Lorentz and polarization effects, and a face-indexed absorption correction was performed for [D-Ala^3]DPDPE (minimum and maximum transmission factors were 0.354 and 0.843). Pertinent physical data are presented in Table 1.

The structures were solved by direct methods with the aid of the program SHELX86[31] and refined on F_o^2 values using the full-matrix least-squares program SHELXL[32] on the full set of independent data as described elsewhere.[33] Refined parameters for both compounds included atomic coordinates and anisotropic thermal parameters for all non-hydrogen atoms in the peptide molecules and for ordered water molecules. Hydrogen atoms, on all peptide molecules, were placed at calculated positions and were allowed to ride on their covalently bonds atoms. Isotropic hydrogen thermal parameters were reset at the end of each refinement cycle to equal 1.1× the U_{eq} value of their covalently bonded atoms (1.2 × U_{eq} for methyl hydrogens). For **2**, the disordered water molecules were refined anisotropically and the sum of occupancies of overlapping water molecules was constrained to 1.0. In **3**, the disordered waters form a solvent channel. Thermal parameters were fixed for the disordered water molecules, and their coordinates and occupancies were refined. A check was performed on the final positions to ensure that the sum of occupancies at any particular water site was not greater than 1.0. In this way 13 independent sites, with a total occupancy of 5.5 water molecules, were used to model the channel. As a further check on the reasonableness of the solvent model, an R_{free} was calculated after each cycle of refinement. R_{free} is the R factor for a set of 85 reflections (every 30th one in the data set) which were omitted from the refinement. Final R factors are listed in Table 1.

NMR Data Acquisition. NMR parameters were obtained from 1D and 2D experiments performed on a BRUKER AM 500 spectrometer equipped with an ASPECT 3000 computer and a 5 mm inverse probehead. Data handling was performed using FELIX 2.0 on a Silicon Graphics 4D/35+ workstation. Peptide samples were dissolved in DMSO-d_6 at a concentration of 15 mg/0.5 mL. All spectra were recorded at 310 K except for the temperature coefficient measurements, which were measured at 5 K increments from 305 to 325 K. Proton and carbon chemical shifts were calibrated to the DMSO-d_6 solvent signal at 2.49 ppm for ^{1}H and 39.5 ppm for ^{13}C. Sequential assignment[34] of proton resonances was achieved by the combined use of z-filtered TOCSY[35] and ROESY[36] experiments. 2D TOCSY spectra

(31) Sheldrick, G. M. *SHELX86—A Program for the Solution of Crystal Structures*; University of Gottingen: Gottingen, Federal Republic of Germany, 1986.

(32) Sheldrick, G. M. *Methods Enzymol*., submitted.

(33) Flippen-Anderson, J. L.; Deschamps, J. R.; Ward, K. B.; George, C.; Houghten, R. *J. Pept. Protein Res*. **1994**, *44*, 97−104.

were recorded in phase-sensitive mode using the TPPI method[37] frequency sign discrimination in the F1 dimension. Isotropic mixing was achieved with the MLEV-17[35e] pulse sequence flanked by two trim pulses. ROESY experiments were performed in inverse mode using the decoupler for ^{1}H pulsing. A CW spin-lock field was applied to establish magnetization transfer between dipolar coupled protons. ROE cross peak intensities were classified as strong (s), medium (m), or weak (w) correlations. ^{1}H chemical shifts and conformationally important homonuclear vicinal coupling constants were extracted from resolution enhanced 1D spectra or from highly digitized 1D traces of 2D *z*-filtered TOCSY spectra.

Proton-detected heteronuclear HMQC and HMQC-TOCSY[38] experiments were used for the assignment of protonated carbon resonances. The rotamer populations of the χ_1 side chain torsion angles of D-Pen residues in DPDPE, [L-Ala^3]DPDPE, and [D-Ala^3]DPDPE were calculated from the long-range heteronuclear $^3J_{H\alpha C\gamma}$ coupling constants. These were measured with a selective variant of the long-range Overbodenhausen (HSQC) experiment.[39] From the measured heteronuclear $^3J_{H\alpha C\gamma}$, $^3J_{H\alpha C\gamma'}$ vicinal coupling constants, the rotamer populations were calculated using the following equations:[40]

$$J_{H\alpha C\gamma} = P\,{}^{ap}J_{H\alpha C\gamma} + (1-P)\,{}^{sc}J_{H\alpha C\gamma}$$

$$J_{H\alpha C\gamma'} = P'\,{}^{ap}J_{H\alpha C\gamma'} + (1-P')\,{}^{sc}J_{H\alpha C\gamma'}$$

where P and P' are rotamer populations corresponding to the antiperiplanar (ap) arrangements of the relevant spins. Values of ${}^{ap}J_{H\alpha C\gamma} = 8.5$ Hz and ${}^{sc}J_{H\alpha C\gamma} = 1.4$ Hz were used for antiperiplanar and synclinal (sc) arrangements.

Molecular Modeling. MD simulations were run on the zwitterionic forms of the X-ray structures of one of the [L-Ala^3]DPDPE conformations and [D-Ala^3]DPDPE in MacroModel 4.5[41] on an Iris 4D/35+ workstation. The simulations were run in the AMBER force field with explicit treatment of all hydrogen atoms. A dielectric constant of $\epsilon = 80.0$ was used to scale down electrostatic interactions in an attempt to implicitly compensate for solvent effects. After assignment of Boltzmann-weighted velocities to all atoms, trajectoris were equilibrated over 10 ps and data were acquired on the molecular motions of the peptides over the next 100 ps. Interproton distances were measured and averaged for each simulation. To form **2** and **3** in the X-ray conformation of DPDPE,[29] the *pro-S* and *pro-R* hydrogens on Gly^3 were respectively converted to methyl groups. After energy minimization MD simulations were run on these conformations as described above.

Results

X-ray Crystal Structures of [L-Ala^3]- and [D-Ala^3]DPDPE. The results of the X-ray studies on **2** and **3** are illustrated in Figures 2 and 3, respectively. There are four independent molecules of [L-Ala^3]DPDPE in the asymmetric unit, all of which have essentially the same conformation (see Figure 4 and torsion angles listed in Table 2). There are no intramolecular hydrogen bonds. The four molecules consist of two "pairs" of molecules, each of which is formed by eight hydrogen bonds linking N1, N3, N4, and N5 of each molecule to the

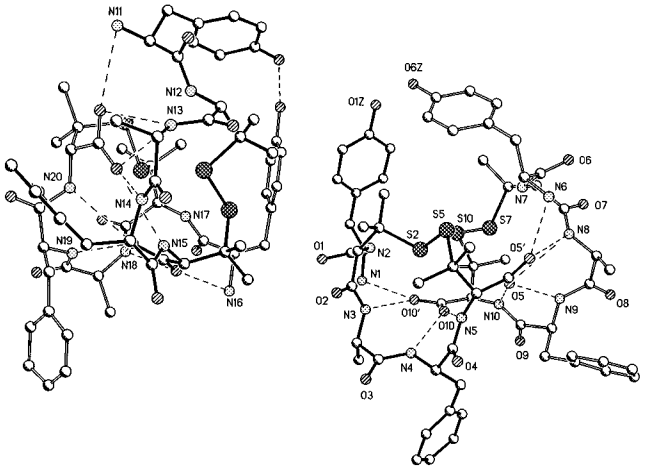

Figure 2. Results of the X-ray study on [L-Ala^3]DPDPE showing the four independent molecules in the asymmetric unit. The figure was drawn using the experimentally determined coordinates. In each "pair" of the molecules, the intermolecular hydrogen bonds are shown as dashed lines and one of the two molecules has been drawn with hollow bonds. In one pair, the nitrogen, oxygen, and sulfur atoms have been labeled, while in the other pair, only the nitrogen atoms are labeled. Hydrogen atoms have been omitted. The overall numbering scheme is the same as that shown in Figure 3 for the D-Ala structure.

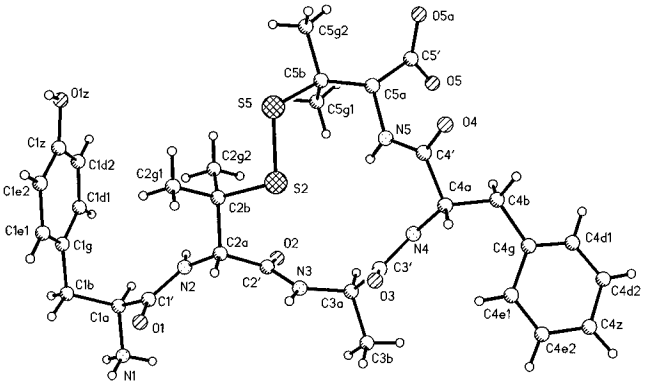

Figure 3. Results of the X-ray study on [D-Ala^3]DPDPE. The figure was drawn using the experimentally determined coordinates. The numbering scheme is also shown. Use the following to relate the labels to atom labels used in the text: a = α, b = β, g = γ, d = δ, e = ϵ, and z = ζ.

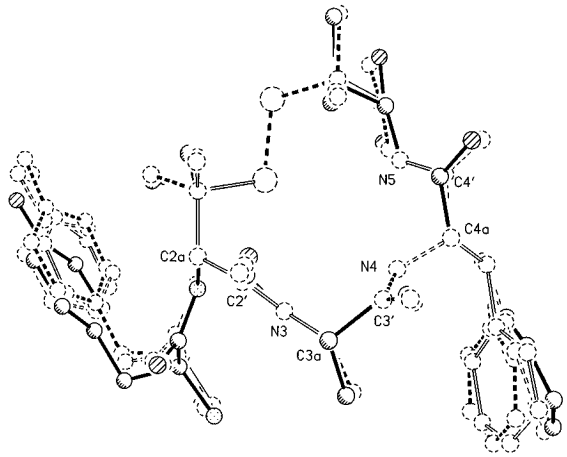

Figure 4. Least-squares fit of the four independent molecules found in the X-ray structure of [L-Ala^3]DPDPE. The atoms used to do the fit are labeled.

(34) Wüthrich, K. *NMR of Proteins and Nucleic Acids*; Wiley: New York, 1986.

(35) (a) Braunschweiler, L.; Ernst, R. R. *J. Magn. Reson.* **1983**, *53*, 521−528. (b) Davis, D. G.; Bax, A. *J. Magn. Reson.* **1985**, *107*, 2820−2821. (c) Subramanian, S.; Bax, A. *J. Magn. Reson.* **1987**, *71*, 325−330. (d) Rance, M. *J. Magn. Reson.* **1987**, *74*, 557−564. (e) Bax, A.; Davis, D. G. *J. Magn. Reson.* **1985**, *65*, 355−360.

(36) (a) Bothner-By, A. A.; Stephens, R. L.; Lee, J.; Warren, C. D.; Jeanloz, R. W. *J. Am. Chem. Soc.* **1984**, *106*, 811−813.

(37) Marion, D.; Wüthrich, K. *Biochem. Biophys. Res. Commun.* **1983**, *113*, 967−974.

(38) (a) Mueller, L. *J. Am. Chem. Soc.* **1979**, *101*, 4481−4484. (b) Lerner, L.; Bax, A. *J. Magn. Reson.* **1986**, *69*, 375−380. (c) Byung-Ha, O.; Westler, W. M.; Markley, J. L. *J. Am. Chem. Soc.* **1989**, *11*, 3083−3085. (d) Kövér, K. E.; Prakash, O.; Hruby, V. J. *J. Magn. Reson.* **1992**, *399*, 426−432.

(39) Kövér, K. E.; Prakash, O.; Hruby, V. J. *Magn. Reson. Chem.* **1993**, *31*, 231−237.

(40) Kessler, H.; Griesinger, C.; Wagner, K. *J. Am. Chem. Soc.* **1987**, *109*, 6927−6933.

(41) Mohamadi, F.; Richards, N. G. J.; Guida, W.; Liskamp, R.; Lipton, M.; Caufield, C.; Chang, G.; Hendrichson, T.; Still, W. C. *J. Comput. Chem.* **1989**, *11*, 440−467.

Table 2. Torsion Angles (deg) for the X-ray Crystal Structure of [L-Ala^3]DPDPE (Four Independent Molecules) and [D-Ala^3]DPDPE

residue	torsion angle[a]	L-Ala^1	L-Ala^2	L-Ala^3	L-Ala^4	D-Ala
Tyr^1	ψ	119	120	131	127	119
	ω	−179	−178	−175	178	−179
	χ^1	−174	−173	−179	179	174
	χ^2	−89	−92	−101	−110	−114
D-Pen^2	φ	73	75	73	79	118
	ψ	12	17	18	12	−137
	ω	−171	−176	−178	−171	−162
(L/D-Ala)^3	φ	−82	−88	−89	−89	124
	ψ	−46	−42	−41	−38	−129
	ω	−172	−169	−168	−172	178
Phe^4	φ	−110	−125	−121	−124	−97
	ψ	−43	−28	−31	−29	−12
	ω	176	176	179	−180	−166
	χ^1	−66	−56	−46	−62	−64
	χ^2	−30	−62	−59	−27	78
D-Pen^5	φ	132	124	122	123	77
S−S bridge	$\chi_2{}^1$	−67	−63	−60	−59	−169
	$\chi_2{}^2$	−165	−175	−174	−173	178
	S−S	113	115	115	112	−111
	$\chi_5{}^1$	−86	−86	−86	−88	68
	$\chi_5{}^2$	67	68	66	71	−79

[a] In S−S bridge: χ^1 = N−Cα−Cβ−S; χ^2 = Cα−Cβ−S−S. In aromatic side chains: χ^1 = N−Cα−Cβ−Cγ; χ^2 = Cα−Cβ−Cγ−Cδ1.

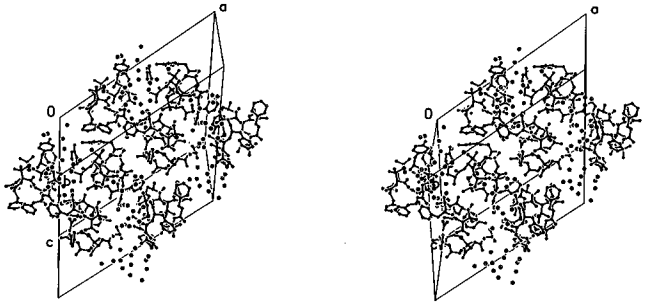

Figure 5. Unit cell packing for [L-Ala^3]DPDPE. The view is drawn looking down the *b* cell axis and shows the distribution of water molecules.

COO^- moiety of its "mate" (see Figure 2 and hydrogen-bond parameters listed in Table 3). In one of two pairs there is also an O1ζ...O1ζ hydrogen bond. Of the N atoms present in the four unique molecules of [L-Ala^3]DPDPE, only the Tyr nitrogen atoms act as donors in hydrogen bonds to peptide molecules outside the asymmetric unit and to water molecules. While all potential oxygen atoms are involved in hydrogen bonding, none of the N2 atoms participates in any hydrogen bonding. There are two types of water molecules cocrystallized with [L-Ala^3]-DPDPE. Approximately one-half of the water molecules in the cell are involved in linking the peptide molecules together. The remaining water molecules form solvent pockets in which the water molecules hydrogen bond extensively with one another but have little interaction with the surrounding peptide molecules (see Figure 5).

[D-Ala^3]DPDPE crystallizes with one peptide molecule and 10 molecules of water in the asymmetric unit. Each peptide molecule is linked to three symmetry-related molecules by 10 peptide−peptide hydrogen bonds (see Table 4) and is also involved in six peptide−water interactions with five water molecules. Of all potential donors and acceptors in the peptide only N5 does not participate in hydrogen bonding. Similarly, in the structure of DPDPE itself,[29] which has three molecules in the asymmetric unit, none of the three independent N5 atoms was a donor in a hydrogen bond. The remaining water molecules form a disordered S-shaped water channel. None of the water molecules in the solvent channel interact directly with the peptide; however, there is an ordered water bridge which connects the channel to the peptide molecules (see Figure 6).

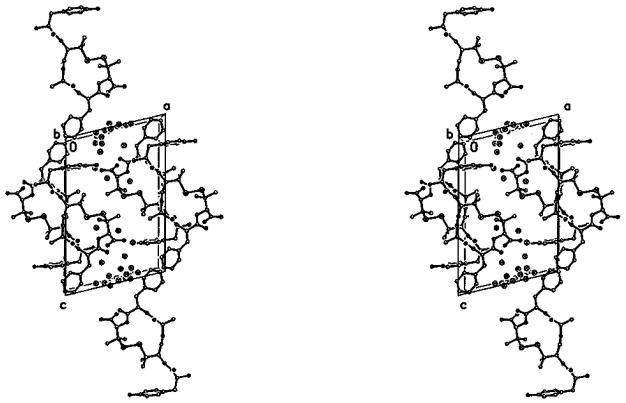

Figure 6. Unit cell packing for [D-Ala^3]DPDPE. This view is drawn to illustrate the water channel aligned along the *b* cell axis.

Solution ^{1}H and ^{13}C NMR Data for DPDPE, [L-Ala^3]-DPDPE, and [D-Ala^3]DPDPE. As has previously been reported for DPDPE,[19] only one time-averaged solution NMR structure was evident on the 1D spectra of **1**, **2**, and **3**. Chemical shift assignments, backbone H−H vicinal coupling constants ($^3J_{H\alpha NH}$), and amide proton chemical shift temperature dependencies for DPDPE, [L-Ala^3]DPDPE, and [D-Ala^3]DPDPE are given in Table 5. In general, the chemical shift and coupling constant data indicate only minor differences between the solution conformations of the three peptides. However, the D-Pen^5 NH is shifted significantly downfield (by 0.77 ppm) in [L-Ala^3]DPDPE when compared to DPDPE and [D-Ala^3]-DPDPE. The amide proton temperature dependencies for D-Pen^5 NH are also distinctly different for the three peptides and suggest greater solvent exposure of this amide proton in [L-Ala^3]DPDPE compared to **1** and **3**. This result mirrors the X-ray data where D-Pen^5 NH is not involved in intra- or intermolecular H-bonding for DPDPE[29] and [D-Ala^3]DPDPE (Figure 3, Table 4). However this amide proton does form a peptide−peptide contact in the unit cell of [L-Ala^3]DPDPE (Figure 2, Table 3), which indicates its availability for interaction with solvent molecules when dispersed in solution.

^{13}C chemical shift values for protonated carbons in **1**−**3** are given in Table 6. Again the chemical shift data are fairly similar for the three peptides in solution. However, consistently higher shift values are observed for the backbone carbon atoms of [L-Ala^3]DPDPE compared to DPDPE and [D-Ala^3]DPDPE. This trend is also seen for the γ carbons of the D-Pen^{2,5} methyl groups (Table 6). Assuming that these effects are due to differences in the disulfide bond region (Table 2, Figure 3 and 4; see Discussion), the rotamer population preferences of the χ_1 torsions of D-Pen residues in **1**−**3** were calculated from the corresponding heteronuclear $^3J_{H\alpha C\gamma}$, $^3J_{H\alpha C\gamma'}$ vicinal coupling constants (Table 7). Populations calculated for **1** and **3** are similar; in each case, χ_1 for D-Pen^2 exhibits approximately equal populations of all three rotamer orientations, with a slight preference for gauche (+). The same is observed for D-Pen^5 in **1** and **3**, with a somewhat increased preference of the gauche-(+) rotamer compared to D-Pen^2. In comparison, the gauche (+) conformation is more than 50% populated on the NMR time scale for both D-Pen^2 and D-Pen^5 in [L-Ala^3]DPDPE. The D-Pen^5 in **2** also exhibits zero population of the trans (t) rotamer, whereas in **1** and **3**, the data are indicative of fairly free rotation about this χ_1 torsion angle.

Qualitative ROE connectivities (in terms of strong, medium, or weak dipolar coupling) are given in Tables 8 and 9 for **2** and **3**, respectively. Again the data do show strong similarities

Table 3. Hydrogen Bonds for [L-Ala^3]DPDPE[a]

donor	acceptor	sym	distance (Å)		donor	acceptor	sym	distance (Å)	
				Peptide−Peptide					
N^1(1)	C=O^2(2)	$-1/2-x$, $1/2+y$, $-z$	2.78	3-centered	N^1(3)	CO$^-$(4)		3.10	
N^1(1)	CO$^-$(2)		2.99		N^3(3)	CO$^-$(4)		3.23	3-centered
N^3(1)	CO$^-$(2)		3.04		N^3(3)	C=O^5(4)		3.19	
N^4(1)	C=O^5(2)		2.72		N^4(3)	C=O^5(4)		2.86	
N^5(1)	C=O^5(2)		3.20		N^5(3)	C=O^5(4)		3.27	
N^1(2)	C=O^2(4)	$-1/2+x$, $-1/2+y$, z	2.87	3-centered	N^1(4)	C=O^2(3)	$1/2-x$, $1/2+y$, $1-z$	2.70	3-centered
N^1(2)	C=O^3(4)	$-1/2+x$, $-1/2+y$, z	3.18		N^1(4)	C=O^5(3)		3.08	
N^1(2)	CO$^-$(1)		2.86		N^3(4)	C=O^5(3)		2.96	3-centered
N^3(2)	CO$^-$(1)		3.19	3-centered	N^3(4)	C=O$^-$(3)		3.27	
N^3(2)	C=O^5(1)		3.19		N^4(4)	CO$^-$(3)		2.67	
N^4(2)	C=O^5(1)		2.79		N^5(4)	CO$^-$(3)		3.13	
N^5(2)	C=O^5(1)		3.27		OH(4)	OH(3)		2.68	
				Peptide−Water (Ordered)					
N^1(1)	W9	$-x$, $1/2+y$, $-z$	2.72		W5	C=O3(3)	$1/2-x$, $1/2+y$, $1-z$	2.84	
N^1(2)	W1		2.75		W6	CO−(1)	$-x$, y, $1-z$	3.06	
N^1(3)	W3		2.70		W6	C=O3(4)	$1/2-x$, $-1/2+y$, $1-z$	2.70	
N^1(3)	W7		3.25		W7	C=O3(1)	$1/2-x$, $1/2+y$, $1-z$	2.67	
N^1(4)	W2		2.74		W7	CO−(4)	$1/2-x$, $1/2+y$, $1-z$	2.75	
N^1(4)	W5		2.82		W9	C=O1(2)	$-x$, y, $-z$	2.72	
OH(1)	W19		2.63		W9	C=O2(4)		3.12	
OH(2)	W20		3.04		W11	C=O4(1)	$-x$, y, $1-z$	2.76	
OH(3)	W4		2.62		W12	C=O1(1)		3.01	
W1	C=O^3(4)	$-1/2-x$, $-1/2+y$, $-z$	3.09		W14	C=O2(2)	$-1/2-x$, $1/2+y$, $-z$	3.10	
W1	C=O^4(4)	$-1/2-x$, $-1/2+y$, $1-z$	2.72		W15	C=O3(3)	$1/2-x$, $1/2+y$, $1-z$	2.89	
W2	C=O^2(1)		2.76		W16	OH(2)	x, $1+y$, z	3.14	
W2	C=O^1(3)	$-1/2-x$, $1/2+y$, $-z$	2.90		W22	C=O3(2)	$-1/2-x$, $1/2+y$, $-z$	2.88	
W3	C=O4(1)		3.13		W23	C=O3(1)		2.89	
W4	C=O4(3)	$1/2-x$, $-1/2+y$, $1-z$	2.66		W27	C=O1(1)		2.93	
				Water−Water					
W1	W10		2.79		W8	W11		2.91	
W3	W3	x, y, $1-z$	3.17		W8	W11	x, y, $1-z$	2.91	
W3	W7		2.73		W15	W22		2.96	
W4	W16	x, $-1+y$, z	2.77		W15	W16		2.95	
W5	W12		2.82		W16	W31	x, $1+y$, z	2.98	
W6	W11		2.65		W27	W27	$-x$, y, $-z$	2.60	
W8	W10		2.61		W31	W31	$-x$, y, $-z$	2.90	

[a] The hydrogen bond approaches between ordered water molecules are listed. There is more than one way to assign distribution of donors and acceptors. There are also several peptide−water and water−water interactions involving the disordered water molecules which are not listed.

Table 4. Hydrogen Bonds for [D-Ala^3]DPDPE

donor	acceptor	sym	distance (Å)
		Peptide−Peptide	
N^1	C=O^5	$2-x$, $1/2+y$, $1-z$	2.74
N^2	C=O^3	$2-x$, $-1/2+y$, $1-z$	2.98
N^3	C=O^2	$2-x$, $1/2+y$, $1-z$	3.05
N^4	C=O^1	$2-x$, $-1/2+y$, $1-z$	2.88
OH	CO$^-$	$1-x$, $1/2+y$, $1-z$	2.61
		Peptide−Water (Ordered)	
N1	W1	$2-x$, $-1/2+y$, $1-z$	2.76
N1	W2		2.80
W1	C=O^4		2.73
W3	OH		2.80
W4	CO$^-$		2.97
W5	OH		2.91
		Water−Water (Ordered)	
W2	W3	$1+x$, y, z	2.80
W3	W4	$1-x$, $-1/2+y$, $1-z$	2.96
W4	W5	$1-x$, $1/2+y$, $1-z$	2.86

between the solution structures of [L-Ala^3]DPDPE and [D-Ala^3]-DPDPE, particularly about the Tyr^1-D-Pen^2 and Phe^4-D-Pen^5 regions. However, different ROE patterns are observed about D/L-Ala^3 in the two peptides. The D-Ala^3 NH in **3** shows a strong ROE to the D-Pen^2 α-proton and a medium ROE to the D-Ala^3 α-proton. In addition, a strong ROE is observed between the D-Ala^3 α-proton and the Phe^4 NH. In comparison, the L-Ala^3 NH in [L-Ala^3]DPDPE exhibits weak contacts with the 2 and 3 position α-protons as well as an additional weak ROE to the Phe^4 NH not seen for peptide **3**. The L-Ala^3 α-proton shows only a medium ROE to the Phe^4 NH. These ROE connectivities indicate opposite orientations of the D-Pen^2-D/L-Ala^3 amide group, consistent with those observed for the X-ray structures of **2** and **3**.

Molecular Dynamics Simulations. Molecular dynamic (MD) simulations of the X-ray structures of **2** and **3** (labeled MD2 and MD3, respectively) were run in order to compare the effects of crystal packing with the dynamic averaged conformational information present in the solution ^{1}H NMR data. MD simulations were conducted in the AMBER force field, with the X-ray coordinates as the starting point and explicit treatment of all hydrogen atoms. After 10 ps of equilibration, data were collected over a 100 ps time period at 300 K. Key interproton distances of backbone hydrogens found to give ROEs in solution were averaged over the simulations and compared with the experimentally observed NMR data (Tables 8 and 9). The conformational stability of the dynamics trajectories was assessed by minimization of all structures collected over the simulation, followed by rms overlay of the backbone atoms in each case which showed that they all differed by less than 1.0 Å from each other and the starting X-ray structure. Also the total internal energy of all simulations had a maximum standard deviation of ≤5.28 kJ/mol (data not shown), indicating that there were no internal energy perturbations due to major conformational transitions throughout each trajectory.

In order to determine whether a component of the solution NMR data was due to a DPDPE (i.e., **1**, Figure 1)-like structure, MD simulations of [L-Ala^3]DPDPE and [D-Ala^3]DPDPE in the

Table 5. ^{1}H Chemical Shift (δ, ppm), Proton Homonuclear Coupling Constants (J, Hz), and Amide Proton Chemical Shift Temperature Dependencies (ppb/K) for DPDPE (**1**), [L-Ala^3]DPDPE (**2**), and [D-Ala^3]DPDPE (**3**) in DMSO-d_6 (temperature coefficients of NH protons are given in parentheses)

	NH			H_α		
residue	**1**	**2**	**3**	**1**	**2**	**3**
Tyr^1				4.25 $J_{\alpha\beta}$ = 9.2, 6.9	4.15 $J_{\alpha\beta}$ = 7.0, 7.6	4.19 $J_{\alpha\beta}$ = 6.3, 8.5
D-Pen^2	8.60 $J_{NH\alpha}$ = 8.5 (−3.2)	8.67 $J_{NH\alpha}$ = 8.7 (−4.4)	8.55 $J_{NH\alpha}$ = 9.2 (−7.8)	4.54	4.26	4.57
Xxx^3	8.57 $J_{NH\alpha}$ = 5.0, 7.9 (−2.6)	8.12 $J_{NH\alpha}$ = 8.3 (−3.7)	8.46 $J_{NH\alpha}$ = 9.2 (−5.7)	3.21, 4.40	4.24 $J_{\alpha\beta}$ = 7.2	4.61 $J_{\alpha\beta}$ = 7.0
Phe^4	8.88 $J_{NH\alpha}$ = 7.0 (−5.1)	8.51 $J_{NH\alpha}$ = 7.8 (−5.5)	8.90 $J_{NH\alpha}$ = 8.2 (−7.0)	4.41 $J_{\alpha\beta}$ = 4.5, 10.2	4.02 $J_{\alpha\beta}$ = 11.0, 5.0	4.31 $J_{\alpha\beta}$ = 3.5, 11.5
D-Pen^5	7.23 $J_{NH\alpha}$ = 8.4 (+0.3)	8.01 $J_{NH\alpha}$ = 8.4 (−3.8)	7.24 $J_{NH\alpha}$ = 8.2 (0.0)	4.33	4.30	4.30

Table 6. ^{13}C Chemical Shifts (δ, ppm) of Protonated Carbons of DPDPE (**1**), [L-Ala^3]DPDPE (**2**), and [D-Ala^3]DPDPE (**3**) and Heteronuclear Coupling Constants between the D-Pen^{2,5} Hα and Cγ and Cγ′ (i.e., β-methyl carbons)

	Cα			Cβ			Cγ		
residue	**1**	**2**	**3**	**1**	**2**	**3**	**1**	**2**	**3**
Tyr^1	53.4	53.8	53.4		36.4	37.1			
D-Pen^2	59.0	62.3	58.3				25.4 $J_{H\alpha C\gamma}$ = 3.6 ± 0.4 27.7 $J_{H\alpha C\gamma}$ = 3.5 ± 0.4	26.3 $J_{H\alpha C\gamma}$ = 3.0 ± 0.4 27.2 $J_{H\alpha C\gamma}$ = 3.0 ± 0.4	25.1 $J_{H\alpha C\gamma}$ = 3.6 ± 0.4 27.6 $J_{H\alpha C\gamma}$ = 3.6 ± 0.4
Xxx^3 [a]	42.0	49.4	47.5	17.4	17.6				
Phe^4	56.1	57.9	55.4	36.4	35.5	36.3			
D-Pen^5	62.0	62.8	62.2				25.6 $J_{H\alpha C\gamma}$ = 3.4 ± 0.4 27.2 $J_{H\alpha C\gamma}$ = 3.3 ± 0.4	26.2 $J_{H\alpha C\gamma}$ = 4.3 ± 0.3 27.2 $J_{H\alpha C\gamma}$ = <1−2	25.4 $J_{H\alpha C\gamma}$ = 3.3 ± 0.4 27.2 $J_{H\alpha C\gamma}$ = 2.7 ± 0.4

[a] Xxx = Gly in **1**, L-Ala in **2**, and D-Ala in **3**.

Table 7. Rotamer Populations of D-Pen^2/D-Pen^5 Residues in DPDPE (**1**), [L-Ala^3]DPDPE (**2**), and [D-Ala^3]DPDPE (**3**) Determined from the Heteronuclear $^3J_{H\alpha C\gamma}$ $^3J_{H\alpha C\gamma'}$ Vicinal Coupling Constants Given in Table 6 (see Methods)

	1		**2**		**3**	
	D-Pen^2	D-Pen^5	D-Pen^2	D-Pen^5	D-Pen^2	D-Pen^5
g (−)	30	27	23	41	31	18
t	31	28	23	0	31	27
g (+)	39	45	54	59	38	55

Table 8. Experimentally Observed ROE Connectivities for [L-Ala^3]DPDPE (**2**) in DMSO-d_6 at 310 K[a]

ROE connectivities		ROE intensity
Pen^2-NH	Tyr^1-α	(m)
	Pen^2-α	(m-w)
	Ala^3-NH	(v.weak)
Ala^3-NH	Pen^2-α	(w)
	Ala^3-α	(w)
	Phe^4-NH	(w)
Phe^4-NH	Ala^3-α	(m)
	Phe^4-α	(m)
	Pen^5-NH	(w)
Pen^5-NH	Pen^5-α	(w)
Tyr^1-α	Tyr^1-β,β′	(m)
	Tyr^1-Ar	(s)
Pen^2-α	Pen^2-γ,γ′	(m)
Ala^3-α	Ala^3-β	(s)
Phe^4-α	Phe^4-Ar	(m)
Pen^5-α	Pen^5-γ,γ′	(m)
Tyr^1-Ar	Tyr^1-β,β′	(m)
Phe^4-Ar	Phe^4-β	(m)
	Ala^3-β	(m)

[a] Relative intensities were determined as strong (s), medium (m), or weak (w).

starting coordinates of the X-ray structure of DPDPE (labeled MD2_DPDPE and MD3_DPDPE, respectively) as reported by Flippen-Anderson et al.[29] were similarly recorded. The average interproton distances between backbone hydrogens with an experimentally observed ROE were calculated over each simulation and are given in Tables 10 and 11. Qualitative ROE intensities were estimated from the average interproton distances, and these were then compared back with the experimental values. For [D-Ala^3]DPDPE, the predicted ROEs are in complete agreement between the MD simulations from the crystal structure of **3** and the X-ray structure of DPDPE. The predicted values are also in close agreement with the experimentally determined intensities (Table 11). However, for [L-Ala^3]DPDPE, there are significant differences in the estimated ROEs between the two trajectories, especially about the L-Ala^3 amide proton. A medium ROE is calculated between L-Ala^3 NH and Phe^4 NH (average interproton distance of 2.61 Å) in the X-ray structure of **2** (MD2), while no ROE is expected between these protons from the MD2_DPDPE simulation (average distance of 4.57 Å, Table 10). Conversely, no ROE is predicted between the L-Ala^3 NH and its α-proton (average distance 4.51) while a medium ROE is estimated for these protons in MD2_DPDPE. Taking the average of these estimated distances from the two simulations predicts a weak ROE in each example discussed above (Table 10, last column), which is in fact what is observed experimentally. Differences in the average potential energy (⟨PE⟩) collected over the trajectories between MD2 and MD2_DPDPE and between MD3 and MD3_DPDPE are given in Table 12.

Table 9. Experimentally Observed ROE Connectivities for [D-Ala^3]DPDPE (**3**) in DMSO-d_6 at 310 K

ROE connectivities		ROE intensity
Pen^2-NH	Tyr^1-α	(s)
	Pen^2-α	(m)
	Pen^2-γ	(m)
Ala^3-NH	Pen^2-α	(s)
	Pen^2-γ'	(w)
	Ala^3-α	(m-w)
	Ala^3-β	(m)
Phe^4-NH	Ala^3-α	(s)
	Phe^4-α	(w)
	Phe^4-β	(m-s)
	Pen^5-NH	(m)
Pen^5-NH	Pen^2-γ	(m)
	Pen^5-α	(m)
	Pen^5-γ,γ'	(m)
Tyr^1-α	Tyr^1-β,β'	(m-w)
Pen^2-α	Pen^2-γ,γ'	(m-s)
Ala^3-α	Ala^3-γ	(s)
Phe^4-α	Ala^3-β	(w)
	Phe^4-β	(s)
	Phe^4-β'	(w)
	Phe^4-Ar	(m)
Pen^5-α	Pen^5-γ,γ'	(m-s)
Phe^4-Ar	Ala^3-β	(w)
	Phe^4-β	(m)
	Phe^4-β'	(w)

[a] Relative intensities were determined as strong (s), medium (m), or weak (w).

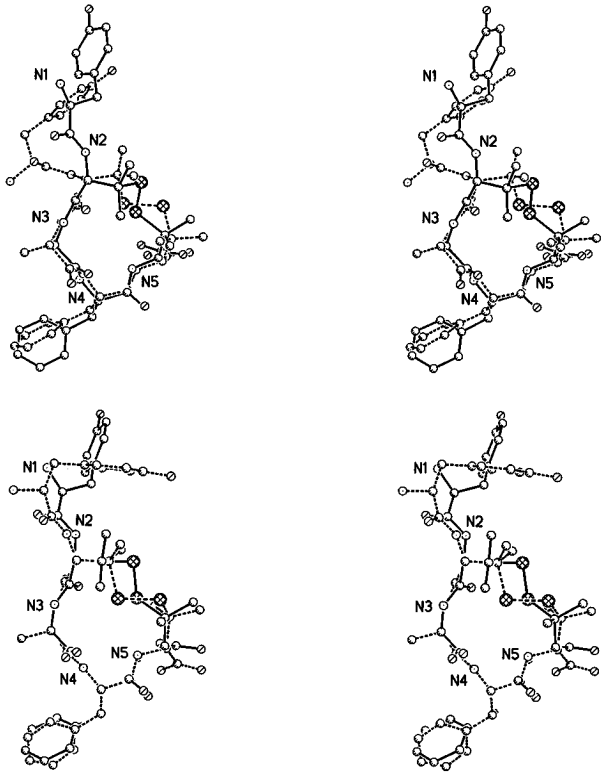

Figure 7. Stereo least-squares fit, drawn from the X-ray coordinates, of (a) [L-Ala^3]DPDPE (dashed lines) to DPDPE and (b) [D-Ala^3]DPDPE (dashed lines) to DPDPE.

Discussion

Comparison of the Conformational Preferences of DPDPE (1), [L-Ala^3]DPDPE (2), and [D-Ala^3]DPDPE (3). Overlays of the previously reported X-ray structure of DPDPE[29] with [L-Ala^3]DPDPE and [D-Ala^3]DPDPE are depicted in Figure 7. The key conformational differences between DPDPE and [L-Ala^3]DPDPE are that they have opposite disulfide bond helicities and that the ψ^2 and φ^3 torsion angles around the amide bond between D-Pen^2 and the position 3 residue are reversed (Figure 7 (top)) between the two X-ray structures. In contrast, the peptide backbones of the X-ray structures of DPDPE and [D-Ala^3]DPDPE are very similar; however, there are differences in orientation about the D-Pen^2 and D-Pen^5 side chains which are both gauche (+) for DPDPE and trans and gauche (−), respectively, for [D-Ala^3]DPDPE. This gives the appearance of opposite disulfide bond helicities for the structures of **1** and **3** when in fact they are the same (Table 2).

When comparing these X-ray structures, it should be noted that some differences may be due to crystal packing forces, rather than true internal conformational preference. This is particularly important in attempting to determine a conformational basis for the biological activity of these peptides. As described in the Introduction, DPDPE is a potent full agonist at the δ opioid receptor. However, while [L-Ala^3]DPDPE has high affinity for the δ receptor, it is only a partial agonist *in vivo* and functionally antagonizes DPDPE at this receptor.[30] This suggests that **1** and **2** adopt different conformations in receptor binding, i.e. agonist and antagonist, respectively, but that [L-Ala^3]-DPDPE can to some minor extent adopt a "DPDPE-like" conformation as an energetically disfavored structure in order to account for its partial agonist behavior. Comparison of the MD simulations of [L-Ala^3]DPDPE in the X-ray structure reported here (MD2) and in the X-ray structure reported for DPDPE[29] (MD2_DPDPE) does indicate that a "DPDPE-like" conformation for **2** is energetically disfavored (Table 12). The ROE data in DMSO solution however are too ambiguous to indicate a preferred orientation of the amide between D-Pen^2 and L-Ala^3 in [L-Ala^3]DPDPE. For example, dipolar contacts are observed between L-Ala^3 NH and both of the D-Pen^2 and Phe^4 NHs, which is consistent with the flipped amide in the [L-Ala^3]DPDPE X-ray structure; also present are ROEs between L-Ala^3 NH and the D-Pen^2 and L-Ala^3 α-protons which are more appropriate for a "DPDPE-like" structure (compare MD2 and MD2_DPDPE, Table 10).

All of the experimentally conflicting ROEs in this region are weak and are in fact better interpreted by assuming the existence of a conformational equilibrium between the X-ray structures of **1** and **2**. As discussed in the Results, simply taking the average of the predicted ROE intensities from both simulations gives a closer correlation with the experimentally determined values than considering each simulation individually (Table 10). The remainder of the backbone ROE contacts calculated in both the MD2 and MD2_DPDPE simulations are very similar to those experimentally observed (Table 10) and hence are consistent with both X-ray structures. The highly qualitative nature of the ROE data presented here as well as that calculated from MD simulation, however, renders an estimation of the relative populations of the two conformations in solution impossible. However, the "DPDPE-like" conformation of [L-Ala^3]DPDPE is predicted to be significantly higher in energy than the X-ray structure of **2** presented here (Table 12) and thus is expected to be less populated, which is consistent with the biological findings.

The backbone residues making up the rings of DPDPE and [D-Ala^3]DPDPE are of virtually identical conformation (Figure 7 (bottom)). The D-Pen^2-D-Ala^3 amide adopts the same orientation in **3** as that observed for D-Pen^2-Gly^3 in DPDPE[29] (Table 2). As discussed above, minor differences in the X-ray structures of **1** and **3** are observed about the χ_1 torsion angles of D-Pen^2 and D-Pen^5, which give the appearance of differing helicities about the disulfide bonds. In contrast, ROEs between the α-protons of D-Pen^{2,5} and their corresponding β-methyl

Table 10. Comparison of Observed and Predicted ROE Intensities for the Backbone Hydrogen Atoms of [L-Ala^3]DPDPE (**2**) in DMSO Solution[a]

ROE connectivities		observed ROE intensity	MD simulations[b] MD2		MD2_DPDPE		predicted ROE intensity
Pen^2-NH	Tyr^1-α	(m)	2.84	(m)	2.78	(m)	(m)
	Pen^2-α	(m-w)	2.92	(m-w)	2.92	(m-w)	(m-w)
	Ala^3-NH	(v.weak)	2.38	(m)	4.64	(no)[c]	(v.weak)
Ala^3-NH	Pen^2-α	(w)	3.46	(w)	2.26	(s)	(m)
	Ala^3-α	(w)	4.51	(no)	2.86	(m)	(w)
	Phe^4-NH	(w)	2.61	(m)	4.57	(no)	(w)
Phe^4-NH	Ala^3-α	(m)	2.52	(m)	3.49	(w)	(m-w)
	Phe^4-α	(m)	2.93	(m-w)	2.93	(m-w)	(m-w)
	Pen^5-NH	(w)	2.39	(m)	2.41	(m)	(m)
Pen^5-NH	Pen^5-α	(w)	3.03	(w)	2.98	(m-w)	(w)

[a] Interproton distances were monitored during MD simulations of **2** with the starting coordinates for its X-ray structure (Table 2; MD2) and the X-ray structure of DPDPE (MD2_DPDPE, ref 29). Distances were averaged over the simulation and classified to give strong (s; less than 2.5 Å), medium (m; 2.5−3.0 Å), and weak (w; 3.0−3.5 Å) ROE intensities. Predicted ROE intensities in the last column are the average of the MD2 and MD2_DPDPE simulations, which more closely resemble the experimental results. [b] Averaged interproton distance and corresponding expected ROE strength. [c] no = predicted no ROE observable.

Table 11. Comparison of Observed and Predicted ROE Intensities for the Backbone Hydrogen Atoms of [D-Ala^3]DPDPE (**3**) in DMSO Solution[a]

ROE connectivities		observed ROE intensity	MD simulations[b] MD3		MD3_DPDPE		predicted ROE intensity
Pen^2-NH	Tyr^1-α	(s)	2.45	(m)	2.74	(m)	(m)
	Pen^2-α	(m)	2.92	(m-w)	2.92	(m-w)	(m-w)
D-Ala^{3}NH	Pen^2-α	(s)	2.24	(s)	2.33	(s)	(s)
	D-Ala^3-α	(m-w)	2.95	(m-w)	2.95	(m-w)	(m-w)
Phe^4-NH	D-Ala^3-α	(s)	2.61	(m)	2.27	(s)	(s)
	Phe^4-α	(w)	2.96	(m-w)	2.94	(m-w)	(m-w)
	Pen^5-NH	(m)	2.33	(s)	2.61	(m)	(s)
Pen^5-NH	Pen^5-α	(m)	2.93	(m-w)	2.94	(m-w)	(m-w)

[a] Monitoring of interproton distances and estimation of corresponding ROE intensity is described in Table 10. [b] Averaged interproton distance and corresponding expected ROE strength.

Table 12. Comparison of the Average Potential Energies, ⟨PE⟩, of MD Simulations of [L-Ala^3]DPDPE (**2**) and [D-Ala^3]DPDPE (**3**)[a]

	⟨PE⟩ (kJ/mol)	Δ⟨PE⟩
MD2	337.8	
MD2_DPDPE	375.9	38.1
MD3	365.7	
MD3_DPDPE	365.3	−0.4

[a] Starting coordinates for the trajectories were taken from the crystal structures reported here (Table 2) for **2** (MD2) and **3** (MD3). MD simulations of **2** and **3** in the starting X-ray coordinates of DPDPE (ref 29) were also made (i.e., labeled MD2_DPDPE and MD3_DPDPE, respectively). The difference in average potential energy (Δ⟨PE⟩ = [MDX_DPDPE] − [MDX]) is also shown.

groups for DPDPE and [D-Ala^3]DPDPE appear to be of approximately equal strength (Tables 8 and 9), implying that there is relatively free rotation about the χ_1 angles of these residues. Measurement of the heteronuclear vicinal coupling constants between Hα and the Cγ's of D-Pen^{2,5} strongly supports these observations and, in fact, indicates a slight preference for the gauche (+) χ_1 rotamer for both penicilliamine residues in both peptides (Table 7). This favored χ_1 angle is consistent with equal intensity ROEs between Hα and the β-methyl groups of these residues. Further evidence for a dynamic equilibrium about the disulfide region of **1** and **3** is found in MD simulations of [D-Ala^3]DPDPE in its X-ray conformation and in the X-ray conformation of DPDPE which exhibit average potential energies within 0.45 kJ/mol (ϵ = 80.0) of each other at 300 K; considering the approximations in these MD simulation, this suggests that the two conformations about the disulfide region in **3** would be both highly populated in solution.

Given the apparent similarity between the crystal and solution structures of DPDPE and [D-Ala^3]DPDPE, the greatly reduced binding and biological activity of the latter peptide is thus due to the R-methyl group on residue 3. Since the two peptides can adopt the proposed agonist conformation,[29] the R-methyl group in **3** must be incompatible with the steric requirements for interaction with opioid receptors.

Conclusion

Agonist versus Antagonist Conformations. The detailed conformational, dynamic, and energetic information gained from the comparison of X-ray, solution NMR, and MD simulation above allows insights into the conformational requirements for agonist and antagonist activity at δ opioid receptors. The X-ray structure of DPDPE is assumed to be representative of the "agonist" conformation for this peptide when binding to the δ opioid receptor.[29] It thus follows that the X-ray structure(s) of [L-Ala^3]DPDPE approximate an "antagonist" conformation for the peptide at the same receptor. The key conformational differences between the two structures are (i) a 180° flip of the amide between D-Pen^2 and L-Ala^3 in **3** relative to the corresponding amide in DPDPE and (ii) opposite helicities about the disulfide bond.

In solution, ROE data indicate that for both DPDPE and [L-Ala^3]DPDPE the disulfide bond and the χ_1 angles of D-Pen^{2,5} are in rapid torsional exchange on the NMR time scale. However, heteronuclear scalar coupling between the D-Pen Hα and Cγ atoms indicates that for [L-Ala^3]DPDPE the gauche (+) χ_1 rotamer is highly preferred for D-Pen^2, while for D-Pen^5, the trans (t) rotamer is predicted to be unpopulated (Table 7). There are hence significant differences in the disulfide region of [L-Ala^3]DPDPE compared to DPDPE. Differences in helicity about a disulfide bond have been linked to agonist versus antagonist conformations in oxytocin analogs.[42−44]

The flipped amide between positions 2 and 3 in [L-Ala^3]-DPDPE points the amide NH "up" with respect to the L-Phe^4 side chain of residues in the ring. In contrast, DPDPE has this amide NH projecting down.[29] This difference in ψ_2 and φ_3 torsion angles may in itself be responsible for antagonism at the δ receptor by denying the receptor an important H-bond that may be crucial for transduction or, conversely, by forming a new H-bond which stabilizes the peptide−receptor complex in a nontransduction state (however, compare results for JOM-13, ref 45). Alternatively this peptide bond rotation also affects the relative positions and orientations of the Tyr^1 and Phe^4 side chains which are important for receptor binding potency and selectivity[46,47] (Figure 7). In the X-ray structures of DPDPE, the Tyr^1 and Phe^4 aromatics are 13.2−15.9 Å apart, while for [L-Ala^3]DPDPE they are only 10.2−12.1 Å apart. Similarly the Phe^4 aromatic to Tyr^1 amino group distance is greater for DPDPE than [L-Ala^3]DPDPE (12.3−13.4 versus 7.5−8.0 Å). The topographical surfaces of **1** and **2** in these conformations are hence significantly different. The peptides may thus bind the δ opioid receptor in different positions and/or orientations at the active site to effect either agonism or antagonism.[48]

Which of these possibilities is reality will be determined by further synthesis and structure analysis, in a manner similar to that described here. The strength of the combined analysis detailed in this report is clear: while the X-ray crystal data give an accurate static image of the peptide, solution NMR and modeling indicate the overall flexibility and local conformations which are accessible around the X-ray conformation which can be important for understanding the nature of receptor interaction, e.g. agonist versus antagonist structure.

Acknowledgment. The Office of Naval Research (J.L.F.) and NIDA Grants DA30018 (J.L.F.) and DA06284 (V.J.H.) are acknowledged for funding. We would like to acknowledge the kind assistance of Dr. Maguy Letulle, Cheryl McKinley, and Margie Colie in the preparation of this manuscript.

Supporting Information Available: Tables listing atomic coordinates, hydrogen coordinates, isotropic and anisotropic displacement parameters, and bond lengths and angles for [L-Ala^3]DPDPE and [D-Ala^3]DPDPE (21 pages). This material is contained in many libraries on microfiche, immediately follows this article in the microfilm version of the journal, can be ordered from the ACS, and can be downloaded from the Internet; see any current masthead page for ordering information and Internet access instructions. All crystal coordinates as well as tables of bond lengths and angles may be retrieved from the Cambridge Crystallographic Data Center, Cambridge University Chemical Laboratory, Cambridge CB2 1EW, England. Tables of anisotropic thermal parameters and structure factors are available from the NRL authors. The coordinates are also available in PDB format, through the LSM home page under the heading neuropeptide structures (URL http://lsm-www.nrl.navy.mil).

JA9531081

(42) Hruby, V. J.; Chow, M.-S.; Smith, D. D. *Ann. Rev. Pharm. Toxicol.* **1990**, *30*, 501−535.
(43) Hruby, V. J. *Oxytocin; Clinical and Laboratory Studies*; Amico, J. A., Robinson, A. G., Eds.; Elsevier Science Publication Biomedical Division: Amsterdam, 1985; pp 405−414.
(44) Hruby, V. J. *Trends Pharmacol. Sci.* **1987**, *8*, 336−339.
(45) Lomize, A.; Flippen-Anderson, J. L.; George, C.; Mosberg, H. I. *J. Am. Chem. Soc.* **1994**, *116*, 429−436.
(46) Hruby, V. J.; Tóth, G.; Gehrig, C. A.; Kao, L.-F.; Knapp, R.; Lui, G. K.; Yamamura, H. I.; Kramer, T. H.; Davis, P.; Burks, T. F. *J. Med. Chem.* **1991**, *34*, 1823−1830.
(47) Tóth, G.; Russell, K. C.; Landis, G.; Kramer, T. H.; Fang, L.; Knapp, R.; Davis, P.; Burks, T. F.; Yamamura, H. I.; Hruby, V. J. *J. Med. Chem.* **1992**, *35*, 2384−2391.
(48) Portoghese, P. S.; Moe, S. T.; Takemori, A. E. *J. Med. Chem.* **1993**, *36*, 2572−2574.